

## PHARMACOLOGY

# Identification of a selective small-molecule inhibitor of type 1 adenylyl cyclase activity with analgesic properties

Tarsis F. Brust,<sup>1</sup> Doungkamol Alongkronrusmee,<sup>1</sup> Monica Soto-Velasquez,<sup>1</sup> Tanya A. Baldwin,<sup>2</sup> Zhishi Ye,<sup>3</sup> Mingji Dai,<sup>3</sup> Carmen W. Dessauer,<sup>2</sup> Richard M. van Rijn,<sup>1</sup> Val J. Watts<sup>1\*</sup>

2017 © The Authors, some rights reserved; exclusive licensee American Association for the Advancement of Science.

Adenylyl cyclase 1 (AC1) belongs to a group of adenylyl cyclases (ACs) that are stimulated by calcium in a calmodulin-dependent manner. Studies with AC1 knockout mice suggest that inhibitors of AC1 may be useful for treating pain and opioid dependence. However, nonselective inhibition of AC isoforms could result in substantial adverse effects. We used chemical library screening to identify a selective AC1 inhibitor with a chromone core structure that may represent a new analgesic agent. After demonstrating that the compound (ST034307) inhibited  $\text{Ca}^{2+}$ -stimulated adenosine 3',5'-monophosphate (cAMP) accumulation in human embryonic kidney (HEK) cells stably transfected with AC1 (HEK-AC1 cells), we confirmed selectivity for AC1 by testing against all isoforms of membrane-bound ACs. ST034307 also inhibited AC1 activity stimulated by forskolin- and  $\text{G}\alpha_s$ -coupled receptors in HEK-AC1 cells and showed inhibitory activity in multiple AC1-containing membrane preparations and mouse hippocampal homogenates. ST034307 enhanced  $\mu$ -opioid receptor (MOR)-mediated inhibition of AC1 in short-term inhibition assays in HEK-AC1 cells stably transfected with MOR; however, the compound blocked heterologous sensitization of AC1 caused by chronic MOR activation in these cells. ST034307 reduced pain responses in a mouse model of inflammatory pain. Our data indicate that ST034307 is a selective small-molecule inhibitor of AC1 and suggest that selective AC1 inhibitors may be useful for managing pain.

## INTRODUCTION

Adenylyl cyclases (ACs) are integrators of signaling through G protein (heterotrimeric guanine nucleotide-binding protein)-coupled receptors (GPCRs). ACs catalyze the production of adenosine 3',5'-monophosphate (cAMP) from adenosine triphosphate (ATP) (1). GPCRs coupled to inhibitory G proteins ( $\text{G}\alpha_{i/o}$ ) generally inhibit ACs, whereas GPCRs coupled to stimulatory G proteins ( $\text{G}\alpha_s$ ) activate ACs. Moreover, because of their regulatory properties, AC isoforms can also be stimulated or inhibited by  $\text{G}\alpha_q$ -coupled receptors and ion channels (1, 2). There are nine isoforms of membrane-bound ACs in humans, each of which exhibits different regulatory properties and expression patterns (3). All membrane-bound ACs are activated by  $\text{G}\alpha_s$ ; however, on the basis of their additional regulatory properties, these ACs can be divided into four different groups (1, 3). Group 1 ACs are AC1, AC3, and AC8, which can be activated by  $\text{Ca}^{2+}$ /calmodulin; group 2 ACs are AC2, AC4, and AC7, which are conditionally activated by  $\text{G}\beta\gamma$  subunits; group 3 ACs are AC5 and AC6, which are inhibited by calcium; and the group 4 AC is AC9, which is relatively insensitive to the small-molecule AC activator forskolin (1–3).

The different regulatory properties and tissue distribution of the membrane-bound ACs suggest that each isoform may serve distinct purposes. The transcripts for the calcium-stimulated ACs, AC1 and AC8, are highly expressed in the hippocampus, which is a brain region associated with learning and memory (3, 4). Behavioral assays with mice lacking both AC1 and AC8 revealed impaired long-term memory in both passive avoidance and contextual learning assays, whereas mice lacking only AC1 or AC8 displayed wild-type-like behaviors (5). However, AC1 knockout mice lose remote contextual memories faster than wild-type mice (6). These studies suggest that AC1 and AC8 have redundant and specific roles in memory.

<sup>1</sup>Department of Medicinal Chemistry and Molecular Pharmacology and Center for Drug Discovery, College of Pharmacy, Purdue University, 575 Stadium Mall Drive, West Lafayette, IN 47907, USA. <sup>2</sup>Department of Integrative Biology and Pharmacology, McGovern Medical School, University of Texas Health Science Center at Houston, Houston, TX 77030, USA. <sup>3</sup>Department of Chemistry and Centers for Cancer Research and Drug Discovery, College of Science, Purdue University, 720 Clinic Drive, West Lafayette, IN 47907, USA.

\*Corresponding author. Email: watts@purdue.edu

Other studies with mice lacking AC1 suggest that inhibitors of AC1 may be useful for treating neuropathic and inflammatory pain and opioid dependence (7–9). Besides the hippocampus, mRNA for AC1 is also expressed in regions of the central nervous system (CNS) associated with pain and nociception, such as the anterior cingulate cortex (ACC) and dorsal horn neurons of the spinal cord (10–12). The development of chronic pain may share some cellular mechanistic features with memory formation and maintenance, that is, strengthening of synapses through long-term potentiation (LTP) (4, 10). The behavioral responses of AC1 knockout mice to inflammatory and neuropathic pain are largely inhibited compared to wild-type animals (8, 10).

Consistent with these animal studies, the small-molecule inhibitor of AC1 activity NB001 has analgesic properties in both inflammatory and neuropathic rodent models of pain (8, 13). NB001 also inhibited LTP in neurons from the ACC and spinal cord but not the hippocampus (13). Despite the promising effects of NB001, it has a few potential drawbacks, including limited selectivity for AC1 versus AC8 and that the actions of NB001 appear to be mediated by indirect inhibition of AC (13, 14). The present study used a screening platform to identify a new selective AC1 inhibitor from a commercially available natural product-derived small-molecule library. The compound identified (ST034307), a chromone derivative, was highly selective for AC1 inhibition when assayed against other AC isoforms. We also investigated the effects of ST034307 on signaling events mediated by the  $\mu$ -opioid receptor (MOR), including AC inhibition,  $\beta$ -arrestin recruitment, and heterologous sensitization of AC. Moreover, we found that ST034307 exerted analgesic effects in a mouse model of inflammatory pain. In summary, we have identified and characterized a potent AC1 inhibitor that has activity in a mouse model of inflammatory pain.

## RESULTS

### Screening of the NDL-3000 Natural Derivatives Library

To find new AC1 inhibitors, we developed a screening platform based on a previous study from our group that identified small-molecule inhibitors of AC2 (15). We also identified W400 as a nonselective AC1

inhibitor from the AC2 inhibitor screen (Fig. 1). W400 served as a positive control for inhibition in our screening platform, producing a ~10-fold reduction in cAMP accumulation in human embryonic kidney (HEK) cells stably expressing AC1 (HEK-AC1) when stimulated with the calcium ionophore A23187 and the AC activator forskolin. A23187 is a calcium ionophore that activates the overexpressed AC1 in this system (15). We assessed the robustness of our screening platform by conducting a  $Z'$  factor analysis using 3  $\mu$ M A23187 + 30 nM forskolin as the maximal response and 30  $\mu$ M W400 (in the presence of 3  $\mu$ M A23187 + 30 nM forskolin) as the minimum response (16). Our screening resulted in a  $Z'$  factor equal to  $0.55 \pm 0.02$  ( $n = 10$ ), confirming that our platform was amenable to drug library screening (17).

We used the NDL-3000 Natural Derivatives Library (TimTec), which is composed of 3040 natural or natural product derivative compounds with diverse chemical structures. Because forskolin, the most widely used compound to interact with ACs, is a natural compound (18), we anticipated that the NDL-3000 Natural Derivatives Library would contain other regulators of AC activity. We screened the library for compounds that inhibit 3  $\mu$ M A23187 + 30 nM forskolin-stimulated cAMP accumulation in HEK-AC1 cells. With the screen, we identified ST034307 and ST072383 (Fig. 1) as inhibitors of AC1 (data S1). In an assay for cell toxicity, neither compound reduced viability below ~85% compared with vehicle-treated cells (Table 1).

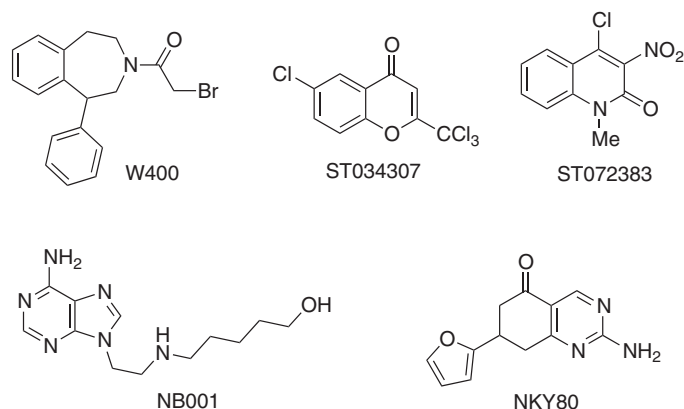


**Fig. 1. Chemical structures of AC1 inhibitors.**

### Selectivity of test compounds against closely related AC1 and AC8 isoforms

We conducted dose-response curves to determine the potencies and maximal effects of the compounds in inhibiting A23187-stimulated cAMP accumulation in HEK cells stably expressing either AC1 or AC8 (Fig. 2, A and B, and Table 1). ST072383 was the more potent of the two inhibitors with a median inhibitory concentration ( $IC_{50}$ ) value of 0.35  $\mu$ M; however, ST072383 also inhibited AC8 (Fig. 2B). Unlike ST072383, ST034307 revealed selective inhibition of AC1. ST034307 actually potentiated AC8 activity to a nonsignificant small extent. We also tested the previously reported AC1 inhibitor NB001 (Fig. 1) in our cell-based AC1 assay and failed to observe any significant inhibition at concentrations up to 30  $\mu$ M (fig. S1). We further tested ST072383 and ST034307 for AC1 inhibition using a second method to measure cAMP accumulation, which produced similar results (table S1).

### Selectivity of test compounds against additional AC isoforms

We tested the selectivity of ST034307 and ST072383 using HEK cells transiently transfected with each of the nine different isoforms of membrane-bound ACs (Fig. 2, C and D). Stimulation of the AC-transfected cells caused a significant increase in cAMP accumulation when compared to the same stimulation paradigms in the Venus-transfected control cells (Fig. 2C). These results indicated that each treatment paradigm provided selective stimulation of the AC isoform that was transfected. ST034307 was selective for inhibition of AC1 in comparison to all other isoforms of membrane-bound ACs (Fig. 2D). We also found that ST034307 potentiated phorbol 12-myristate 13-acetate (PMA)-stimulated cAMP production by AC2 (Fig. 2D). A small potentiation of forskolin-stimulated AC5 and AC6 was also observed. In contrast, ST072383 inhibited all ACs, except for AC5 under the conditions tested. The P-site inhibitor NKY80 significantly inhibited the activity of AC1, AC2, AC3, AC4, AC5, AC6, and AC7, as well as endogenous ACs in the Venus-transfected cells.

### Mechanistic insights on ST034307

We explored the AC inhibition by ST034307 in various cellular and in vitro contexts. The first set of assays conducted included inhibition of AC1 activation by forskolin and  $G_{\alpha_s}$ -coupled receptors. To induce stimulation of AC1 through  $G_{\alpha_s}$ -coupled receptors, we activated the endogenous  $\beta$ -adrenergic receptors in HEK cells with isoproterenol. ST034307 significantly inhibited the forskolin- or isoproterenol-stimulated AC1 activity in HEK cells stably expressing AC1 (Fig. 3A). In contrast,

**Table 1. Inhibition of A23187-stimulated AC1 or AC8 activity and cell toxicity of hit compounds.** Compounds were tested for inhibition of 3  $\mu$ M A23187-stimulated cAMP accumulation in HEK-AC1 or HEK-AC8 cells.  $IC_{50}$  values are presented in  $\mu$ M with 95% confidence interval (CI), and percent inhibition (with 100% set to the basal cAMP) with SEM are reported. We also report the cell toxicity results as a percentage of the vehicle-treated cells. The data in the table represent the average of at least three independent experiments conducted in duplicate. NIO, no inhibition observed.

Compound	HEK-AC1		HEK-AC8		Cell viability
	$IC_{50}$ (95% CI)	% Inhibition (SEM)	$IC_{50}$ (95% CI)	% Inhibition (SEM)	% Vehicle (SEM)
ST072383	0.3 (0.2–0.4)	113 ( $\pm$ 4)	1.6 (0.5–5.7)	55 ( $\pm$ 9)	97 ( $\pm$ 3)
ST034307	2.3 (1.2–4.5)	108 ( $\pm$ 10)	NIO	NIO	85 ( $\pm$ 6)

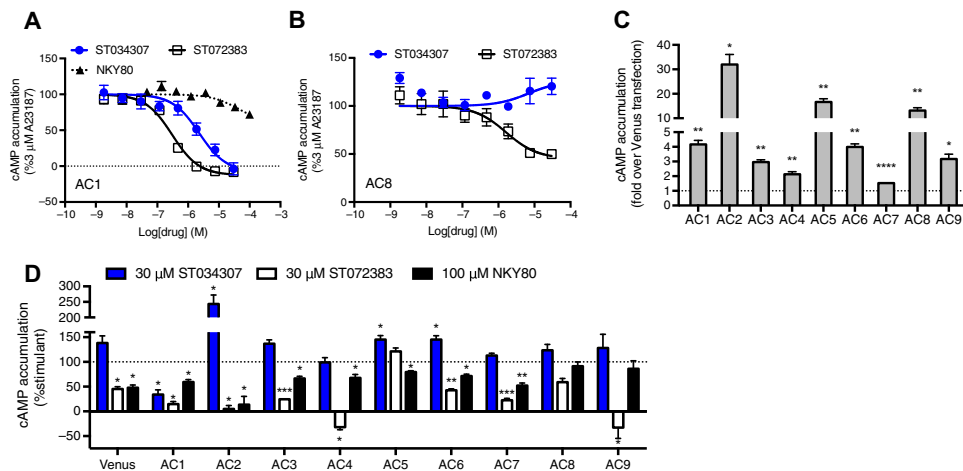


**Fig. 2. Inhibitory activity of ST034307 and ST072383 for AC isoforms.** (A) Inhibition of 3  $\mu$ M A23187-stimulated cAMP accumulation in stably transfected HEK-AC1 cells. (B) Inhibition of 3  $\mu$ M A23187-stimulated cAMP accumulation in stably transfected HEK-AC8 cells. (C) Stimulation of HEK cells transiently transfected with Venus control plasmid or AC isoforms. AC1- and AC8-transfected cells were stimulated with 3  $\mu$ M A23187; AC2-transfected cells were stimulated with 1  $\mu$ M PMA; AC3-transfected cells were stimulated with 30  $\mu$ M forskolin; AC4-transfected cells were stimulated with 10  $\mu$ M isoproterenol; AC5- and AC6-transfected cells were stimulated with 1  $\mu$ M forskolin; AC7-transfected cells were stimulated with 1  $\mu$ M PMA + 1  $\mu$ M forskolin in the presence of transfected  $G\alpha_s$ ; AC9-transfected cells were stimulated with 100 nM isoproterenol in the presence of transfected  $G\alpha_s$ . Y axis represents the cAMP accumulation when compared to the same transfection and stimulation condition in matched Venus-transfected control cells. One-sample *t* test with Bonferroni correction was carried out for statistical analyses. \**P* < 0.05, \*\*\**P* < 0.01, \*\*\*\**P* < 0.0001 compared to the same transfection and stimulation condition in matched Venus-transfected control cells (*n* = 3 to 4). (D) Inhibition of cAMP accumulation in the transiently transfected HEK cells using the indicated concentration of inhibitor. Cells were transfected and stimulated as described in (C). The Venus-transfected HEK cells were stimulated with 30  $\mu$ M forskolin. One-sample *t* test with Bonferroni correction was carried out for statistical analyses. \**P* < 0.05, \*\**P* < 0.01, \*\*\**P* < 0.001 compared to vehicle-treated cells (in the absence of inhibitor, *n* = 3 to 4). In (A), (B), and (D), data were normalized by defining the cAMP levels from activator treatment (without inhibitor) as 100% and baseline cAMP levels as 0%. All data shown represent the average and SEM of at least three independent experiments conducted in duplicate or triplicate.

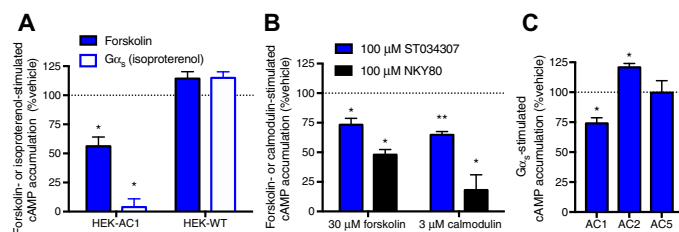


**Fig. 3. Specificity and activity of ST034307 in cells and membrane preparations.** (A) HEK-AC1 and nontransfected HEK cells (HEK-WT) were treated with 30  $\mu$ M ST034307 and stimulated with 300 nM forskolin or 10  $\mu$ M isoproterenol. (B) Cellular membranes from HEK-AC1 cells were isolated, and cAMP production was stimulated with either 30  $\mu$ M forskolin or 3  $\mu$ M calmodulin in the presence of 10  $\mu$ M free  $Ca^{2+}$  with or without either of the indicated AC inhibitors. (C) Cellular membranes from Sf9 cells expressing AC1, AC2, or AC5 were isolated, and cAMP accumulation was stimulated with 50 nM  $G\alpha_s$  in the presence of 100  $\mu$ M ST034307. The data were normalized by defining the cAMP levels from activator treatment (without inhibitor) as 100% and baseline cAMP levels as 0%. All data shown represent the average and SEM of at least three independent experiments conducted in duplicate or triplicate. One-sample *t* test with Bonferroni correction was carried out for statistical analyses. \**P* < 0.05, \*\**P* < 0.01 compared to vehicle-treated cells or membranes (in the absence of inhibitor).

ST034307 had no significant effects in the wild-type HEK cells (Fig. 3A). Although wild-type HEK cells endogenously express mRNA for AC1, no  $Ca^{2+}$ -stimulated cAMP response is observed (19, 20). Thus, the  $G\alpha_s$ - or

forskolin-stimulated cAMP in the wild-type cells reflected the activation of the other endogenous AC isoforms that include AC3, AC5, AC6, AC7, and AC9 (20). These observations further support the fact that the actions of ST034307 involve signaling through AC1, rather than indirect interference with receptor-mediated signaling events upstream of AC. To confirm that ST034307 was not inhibiting AC1 through the effects on  $G\beta\gamma$  or  $G\alpha_{i/o}$ , we tested the inhibition of AC1 activity in HEK-AC1 cells also expressing  $\beta$ ARK-CT, which is the C-terminal portion of GRK2 (G protein-coupled receptor kinase 2) and sequesters  $G\beta\gamma$  (21), or treated with pertussis toxin to block  $G\alpha_{i/o}$  signaling. Neither sequestering  $G\beta\gamma$  subunits with  $\beta$ ARK-CT nor inactivating  $G\alpha_{i/o}$  signaling with pertussis toxin affected ST034307-mediated AC1 inhibition (fig. S2). Together, these observations further support that ST034307 inhibited AC1 directly.

To confirm that the inhibitor was not interfering with a downstream process and required membrane-bound proteins for activity, we also performed *in vitro* assays for AC1 inhibition using cellular membranes isolated from HEK-AC1 cells. We stimulated AC1 activity in membranes with forskolin or purified calmodulin and used the nonselective AC inhibitor NKY80 (Fig. 1) as a control

(14, 15). ST034307 modestly, but significantly, inhibited both the calmodulin- and the forskolin-stimulated AC1 activity in the membranes (Fig. 3B). Further support for AC1 as the direct target of ST034307 was provided by testing for inhibition of AC activity in membranes from Sf9 insect cells expressing recombinant AC1, AC2, or AC5 (14, 15). As in the cell-based assays, ST034307 inhibited AC1 activity (~30%), suggesting a direct mode of inhibition (Fig. 3C). As we observed for the HEK cells, ST034307 also potentiated AC2. The compound was inactive at AC5 even at 100  $\mu$ M.

P-site inhibitors (a class of noncompetitive and uncompetitive AC inhibitors) display higher inhibitory activity when the AC is activated (the higher the activity of the AC, the more robust the AC inhibition by P-site inhibitors) (3, 22, 23). Therefore, we measured inhibition of AC1 activity by ST034307 in response to increasing concentrations of the AC1 activators A23187 and forskolin (fig. S3). Increase in the concentration of A23187 resulted in an increase in the efficacy of inhibition of AC1 by the P-site inhibitor NKY80 (Fig. 4A). In contrast, as the concentration of AC1 activators increased, there was no change (A23187) or a decrease (forskolin) in the efficacy of inhibition by ST034307 (Fig. 4), suggesting that ST034307 is not a P-site inhibitor.

We assessed the activity of ST034307 in a more physiologically relevant system, the hippocampus. We stimulated hippocampal homogenates prepared from C57BL/6 mice with purified calmodulin in the presence of 10  $\mu$ M free  $Ca^{2+}$ . The addition of  $Ca^{2+}$ /calmodulin caused a significant increase in cAMP accumulation in these neuronal homogenates,

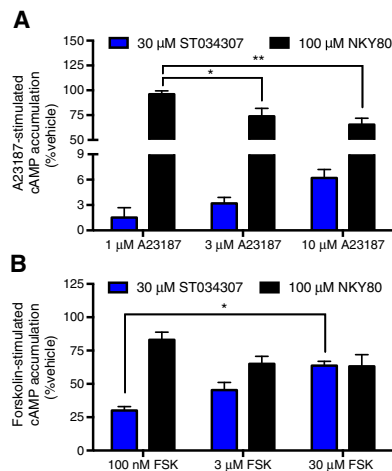


**Fig. 4. Mechanistic insights regarding ST034307.** (A) Inhibition of A23187-stimulated cAMP accumulation in HEK-AC1 cells. (B) Inhibition of forskolin (FSK)-stimulated cAMP accumulation in HEK-AC1 cells. The data were normalized by defining the cAMP levels from activator treatment (without inhibitor) as 100% and baseline cAMP levels as 0%. All data shown represent the average and SEM of at least three independent experiments conducted in triplicate. Data were analyzed using two-way analysis of variance (ANOVA) followed by Tukey's multiple comparisons test. \* $P < 0.05$ , \*\* $P < 0.01$  between indicated concentrations.

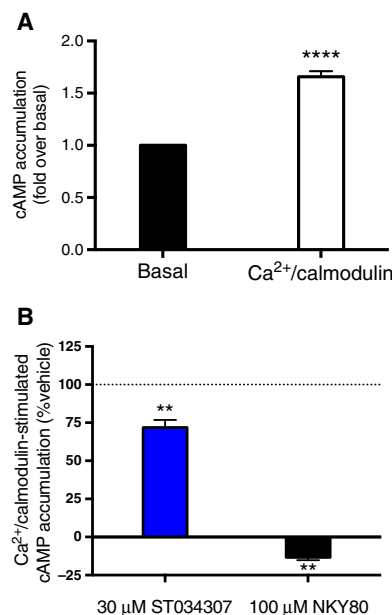


**Fig. 5. Inhibition of  $\text{Ca}^{2+}$ /calmodulin-stimulated cAMP accumulation in hippocampal homogenates.** (A) Mouse hippocampal homogenates were stimulated with 3  $\mu\text{M}$  calmodulin in the presence of 10  $\mu\text{M}$  free  $\text{Ca}^{2+}$  with basal cAMP activity in the absence of  $\text{Ca}^{2+}$ /calmodulin set at 1. (B) Hippocampal homogenates were stimulated with  $\text{Ca}^{2+}$ /calmodulin in the presence of ST034307 or NKY80. Data are normalized to the response in the absence of the inhibitors (3  $\mu\text{M}$  calmodulin + 10  $\mu\text{M}$  free  $\text{Ca}^{2+}$  was defined as 100%, and baseline cAMP levels were defined as 0%) and represent the average and SEM of six independent experiments conducted in triplicate. One-sample  $t$  test for (A) and one-sample  $t$  test with Bonferroni correction for (B). \*\* $P < 0.01$ , \*\*\* $P < 0.001$ , \*\*\*\* $P < 0.0001$  compared to basal or vehicle-treated homogenates (in the absence of inhibitor).

supporting the presence of calcium-stimulated ACs (Fig. 5A). ST034307 significantly inhibited the  $\text{Ca}^{2+}$ /calmodulin-stimulated cAMP accumulation in the hippocampal homogenates (Fig. 5B). The presence of AC1,

AC8, and other AC isoforms in the hippocampus (3, 4) likely explains the more robust inhibition of  $\text{Ca}^{2+}$ /calmodulin-stimulated cAMP accumulation by the nonselective AC inhibitor NKY80 (14) compared to inhibition by the AC1-selective inhibitor ST034307.

### Effects of ST034307 on MOR signaling

Inhibition of ACs may play an important role in the analgesic effects of agonists of the MOR, which is a  $G_{\alpha_{i/o}}$ -coupled receptor that is present with AC1 in areas of the nervous system that are linked to pain and nociception (the dorsal horn of the spinal cord and ACC) (10–12, 24–27). Thus, we investigated the effects of ST034307 on MOR signaling in HEK-AC1 and Chinese hamster ovary (CHO) cells stably expressing MOR. Upon agonist binding, MOR activates G proteins, which inhibit ACs (including AC1), and also recruits  $\beta$ -arrestins, which can lead to additional signaling events or signal termination (28). We exposed HEK-AC1/MOR cells to the MOR agonist DAMGO, ST034307, or both compounds for 1 hour. Exposure to ST034307 enhanced MOR-mediated inhibition of AC1 in HEK-AC1/MOR cells (Fig. 6A). To assess potential effects of ST034307 on  $\beta$ -arrestin recruitment to MOR, we used a commercial assay platform from DiscoverX that is available in genetically engineered CHO cells expressing recombinant MOR and  $\beta$ -arrestin 2 fused to enzyme complementation partners, enabling the detection of interactions between receptor and arrestin. Exposing cells to ST034307 for 30 min before DAMGO or vehicle addition had no effects on the recruitment of  $\beta$ -arrestin to MOR in the CHO-MOR  $\beta$ -arrestin cells (Fig. 6B).

Prolonged activation of the MOR leads to a cellular adaptive response termed heterologous sensitization, which results in the superactivation of AC and has been linked to opioid dependence (29–33). A 2-hour exposure to DAMGO produced a 250% enhancement of A23187-stimulated cAMP accumulation in HEK-AC1/MOR cells when compared to vehicle-treated cells (Fig. 6C). We examined the effects of ST034307 on MOR-mediated heterologous sensitization of AC1 in two different paradigms. To determine the effects of ST034307 on the development of heterologous sensitization, we added ST034307 before the initial activation of the MOR (Fig. 6D). To study the effects of ST034307 on the maintenance of heterologous sensitization, we added ST034307 after persistent activation of the MOR (Fig. 6D). ST034307 dose-dependently inhibited both the development and the maintenance of MOR-mediated sensitization of AC1 (Fig. 6D).

### Analgesic properties of ST034307 in mice

Although we did not test for an effect on ACC neurons or spinal cord neurons in culture, we assayed to determine whether ST034307 has analgesic properties using a mouse model of inflammatory pain. We injected Complete Freund's Adjuvant (CFA) into the hindpaw of mice to induce inflammation and measured pain as hypersensitivity to touch by von Frey filaments (24, 34). Intrathecal injections (into the spinal canal) with ST034307 at doses as low as 0.25  $\mu\text{g}$  caused a significant relief of CFA-induced inflammatory pain, as indicated by the increase in the amount of pressure the mouse tolerated before removing the paw (Fig. 7). As a control pain reliever, we administered DAMGO at 50 ng per mouse (34), which provided a similar reduction in the hypersensitivity response (Fig. 7A). Limited dose-response experiments with ST034307 in this mouse pain model suggested an estimated median effective dose ( $\text{ED}_{50}$ ) value for analgesia of 0.28  $\mu\text{g}$  (Fig. 7B).

To show that an increase in cAMP contributed to the CFA-induced hypersensitivity, we used the nonselective AC activator forskolin. Because forskolin activates all isoforms of AC (except for AC9), we

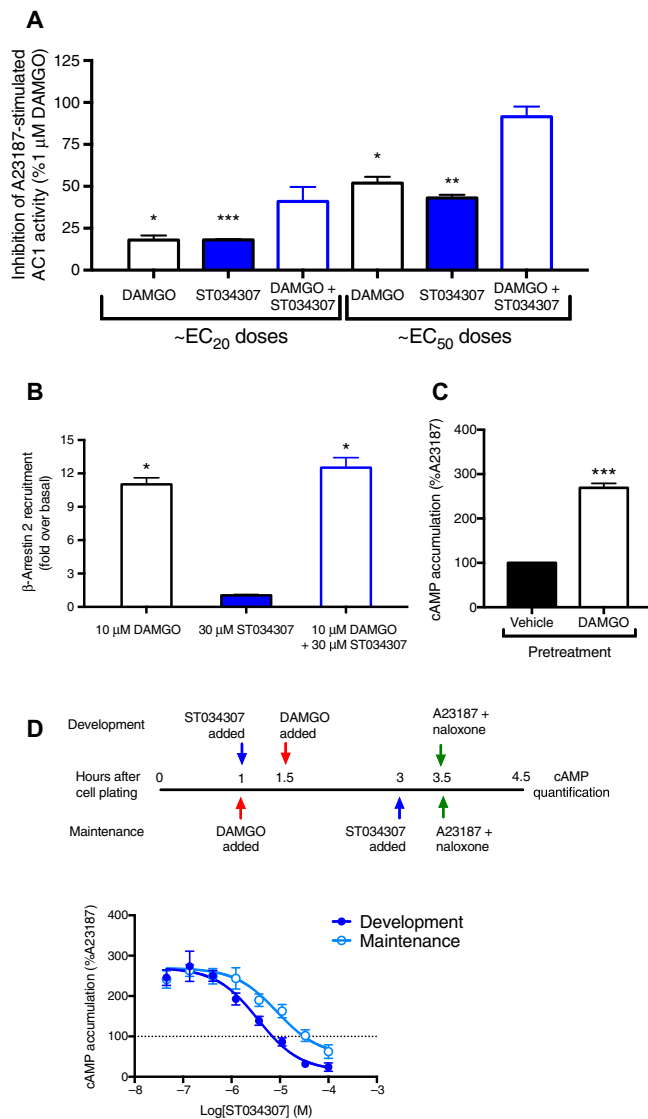


**Fig. 6. Effects of ST034307 on MOR signaling.** (A) Inhibition of A23187-stimulated cAMP accumulation in HEK-AC1/MOR cells. Approximate EC<sub>20</sub> concentrations of ST034307 (0.5 μM) and DAMGO (4 nM) or EC<sub>50</sub> concentrations of ST034307 (7.5 μM) and DAMGO (15 nM) were added alone or in combination as indicated, and cAMP accumulation was measured. Data were normalized by defining the inhibitory response to 1 μM DAMGO in the presence of 3 μM A23187 as 100% and the cAMP response to 3 μM A23187 as 0%. (B) β-Arrestin 2 recruitment in CHO-MOR cells that were treated with 10 μM DAMGO, 30 μM ST034307, or DAMGO + ST034307. (C) Heterologous sensitization of AC1 by the MOR was achieved by pretreating the cells with 1 μM DAMGO for 2 hours and subsequently stimulating cAMP accumulation with A23187 (3 μM) in the presence of naloxone (1 μM). (D) Effects of ST034307 on the development and maintenance of DAMGO-stimulated heterologous sensitization. Timeline of the drug treatments conducted for determining the effects of ST034307 on the development (top) and maintenance (bottom) of DAMGO-induced heterologous sensitization of AC1 (shown in graph below). After drug pretreatment, heterologous sensitization was triggered by the addition of A23187 (3 μM) in the presence of naloxone (1 μM). The data in (C) and (D) were normalized to vehicle-treated cells under basal conditions (0%) or stimulated with A23187 in the presence of naloxone (100%). The data shown represent the average and SEM of at least three independent experiments conducted in duplicate. One-sample *t* test with Bonferroni correction was carried out for statistical analyses in (A), (B), and (C). For (A), \**P* < 0.05, \*\**P* < 0.01, and \*\*\**P* < 0.001 compared to respective DAMGO + ST034307 column; for (B) and (C), \**P* < 0.05 and \*\*\**P* < 0.001 compared to vehicle-treated cells (in the absence of any drugs).

anticipated that forskolin treatment would increase cAMP accumulation at the site of action of ST034307 and, therefore, prevent or impair its analgesic actions. Co-injection of forskolin with ST034307 completely inhibited the analgesic response caused by ST034307 in our inflammatory pain model (Fig. 7C).

## DISCUSSION

Several studies have uncovered the unique physiological functions of AC1 and informed on the clinical potential of compounds targeting this protein (7–9, 13, 35, 36). In mice lacking AC1, acute pain responses such as mechanical pressure and noxious heating were unchanged, whereas behaviors associated with chronic and inflammatory pain were largely inhibited (36). Inspired by these studies, Wang *et al.* (13) identified NB001 as a small molecule that inhibits AC1 activity with an about 10-fold selectivity over AC8.

To identify additional selective inhibitors, we designed and performed a chemical library screen to identify potential AC1 inhibitors. Our efforts resulted in the discovery of a potent and selective AC1 inhibitor (ST034307; IC<sub>50</sub>, 2.3 μM; 95% CI, 1.2 to 4.5 μM). ST034307 is a chromone-derived small molecule with CNS drug-like physicochemical properties (37): molecular weight, 298; CLogP, 4.07; Topological Polar Surface Area, 26; 4 hydrogen bond acceptors and 0 hydrogen bond donors. Multiple types of models (HEK cells expressing AC1-AC9, HEK-AC1, and Sf9-AC1 cell membranes and mouse hippocampal homogenates) and stimulation paradigms (A23187, calmodulin, forskolin, G<sub>α<sub>s</sub></sub>, and G<sub>α<sub>i</sub></sub>-coupled receptor) were used to confirm the activity and selectivity of ST034307. We also examined the effects of ST034307 on acute and chronic MOR signaling in heterologously expressing cells and confirmed its ability to induce analgesia in a mouse inflammatory pain model.

The molecular mechanisms involved in the analgesic properties of AC1 inhibition have been associated with the requirement of cAMP for synaptic plastic changes like LTP (4, 10, 13). The development of chronic pain has been linked to the strengthening of synapses through LTP in the ACC and the spinal cord (4, 10). It has been hypothesized that NMDA (*N*-methyl-D-aspartate) receptor-mediated Ca<sup>2+</sup> influx in neurons from these regions of the nervous system causes AC1 activation, which provides the cAMP required for LTP (10). NB001-mediated inhibition of LTP in the ACC and spinal cord, but not the hippocampus, is consistent with this hypothesis and also with the AC1 knockout models that point to analgesia without notable memory impairments (5, 6, 8, 9, 11, 13).

Of concern for any AC1 inhibitor is specificity because double-knockout mice lacking both AC1 and AC8 present behaviors consistent with severe memory impairments (5, 10). Therefore, one main requirement for an AC1 inhibitor to be used in the treatment of pain is selectivity for AC1 versus AC8. ST034307 did not display any inhibition of AC8 at doses up to 30 μM, revealing marked selectivity for inhibition of AC1 versus AC8. Furthermore, ST034307 did not inhibit any of the other isoforms of AC. The robust potentiation of PMA-stimulated AC2 activity and the modest potentiation of AC5 and AC6 were somewhat unexpected and may reflect a conserved binding site, such as the forskolin binding site at which forskolin analogs can have either stimulatory or inhibitory activity at individual AC isoforms (38). Because there are no genetic knockout rodent models for AC2, it is difficult to predict the physiological consequences of potentiating PMA-mediated AC2 activity (15, 39). PMA activates AC2 through protein kinase C, and AC2 transcripts are expressed in skeletal muscle, in which increased cAMP is

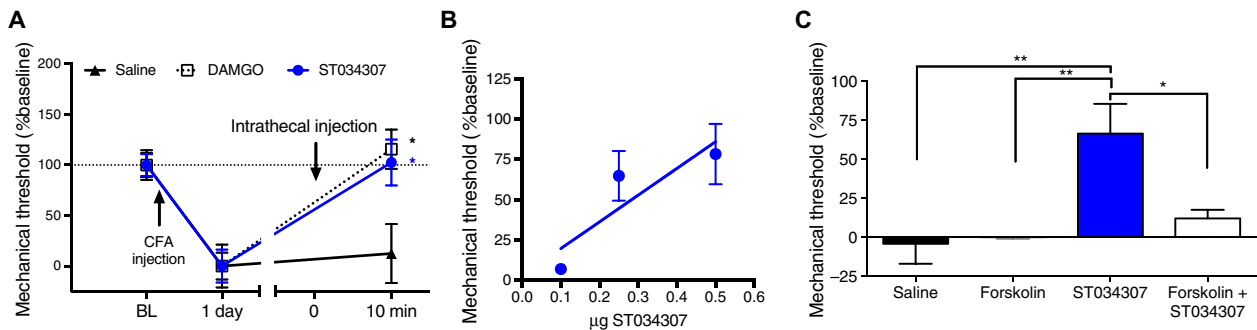


**Fig. 7. Analgesic properties of ST034307 in a mouse model of inflammatory pain.** (A) On day 0, baseline (BL) measurements of mechanical sensitivity of C57BL/6 mice to von Frey filaments were recorded, and inflammatory hypersensitivity was induced by injection of CFA to the hindpaw. On day 1, inflammatory hypersensitivity was measured by von Frey test. Animals received intrathecal injections with saline ( $n = 10$ ), 50 ng of MOR-selective agonist DAMGO ( $n = 11$ ), or 0.5  $\mu\text{g}$  of ST034307 ( $n = 11$ ), and inflammatory hypersensitivity was measured again.  $*P < 0.05$  compared to saline injection at 10 min, analyzed by one-way ANOVA. (B) Dose-response experiments with ST034307 ( $n = 6$  for each condition). Estimated  $\text{ED}_{50}$  value for analgesia of 0.28  $\mu\text{g}$  (95% CI, 0.13 to 0.43;  $n = 6$ ). (C) One day after CFA-induced inflammatory pain, animals received intrathecal injections with saline ( $n = 9$ ), 10  $\mu\text{g}$  of forskolin ( $n = 8$ ), 0.5  $\mu\text{g}$  of ST034307 ( $n = 9$ ), or 10  $\mu\text{g}$  of forskolin + 0.5  $\mu\text{g}$  of ST034307 ( $n = 8$ ), and mechanical hypersensitivity was measured by von Frey test 10 min after injections.  $*P < 0.05$ ,  $***P < 0.01$  compared to each corresponding treatment, analyzed by one-way ANOVA with Tukey's test. The data shown represent the average and SEM of each group of measurements to stimulation of the ipsilateral hindpaw of the mice. All data were normalized by defining the baseline measurements as 100% and the CFA-induced hypersensitivity as 0%.

linked to muscle hypertrophy, repair, and regeneration (15, 40, 41). Efforts to identify ST034307 analogs with greater overall selectivity are currently under way. The activity of ST034307 was not associated with  $\text{G}\beta\gamma$  subunit signaling because sequestering  $\text{G}\beta\gamma$  subunits with  $\beta\text{ARK-CT}$  failed to alter its effects on AC1. Similarly,  $\text{G}\alpha_{i/o}$  activity was ruled out because ST034307-mediated AC1 inhibition was not altered by overnight pertussis toxin pretreatment. These observations and the selectivity of AC1 inhibition versus AC2-AC9 suggested that the actions are unique to AC1 and did not involve a more general inhibition of AC activity through G protein subunits or through modulation of cAMP accumulation or degradation.

One important caveat with the previously described AC1 inhibitor, NB001, is that this compound does not inhibit AC1 in *in vitro* assays performed with cellular membranes (14). These studies indicated that NB001 is not a direct AC1 inhibitor and may act through a distinct mechanism to inhibit AC1 activity in intact cells (14). The present study revealed that, unlike NB001, ST034307 had modest, but significant, inhibitory effect in studies using cellular membranes from HEK or Sf9 cells expressing AC1. ST034307 showed a similar degree of inhibition (~30%) to forskolin-,  $\text{G}\alpha_s$ -, and calmodulin-stimulated AC1 activity. These observations suggested that ST034307 acts, in part, through a mechanism that targets membrane-associated AC1 activity, which is consistent with a direct interaction of ST034307 with AC1. Subsequent cell-based assays using increasing concentrations of AC1 activators suggested that ST034307 is not a P-site inhibitor and that it apparently acts through a distinct mechanism to inhibit AC1, which may partly explain the high selectivity of the compound.

MOR, which has long been targeted for analgesia and antinociception, is also present in the dorsal horn of the spinal cord and ACC (10–12, 24–27). Similar to numerous GPCRs, there are several different signaling pathways activated by MOR (42, 43). MORs couple to  $\text{G}\alpha_{i/o}$  to inhibit ACs and can also lead to signaling events through  $\text{G}\beta\gamma$  subunits, as well as through  $\beta$ -arrestins (42, 44, 45). Biased agonists selectively activate specific signaling pathways downstream of a GPCR (46–49). Notably, several studies have suggested that activation of G proteins by the MOR is linked to the therapeutic analgesia of opioids, whereas activation of  $\beta$ -arrestins is associated with many of the undesired side effects of these drugs, including tolerance, constipation,

and respiratory depression (29, 50–52). Although  $\text{G}\beta\gamma$ -mediated activation of GIRK (G protein-coupled inwardly rectifying potassium) channels has been associated with MOR-induced antinociception, it is intriguing and encouraging that both  $\text{G}\alpha_{i/o}$  and  $\text{G}\beta\gamma$  subunits can inhibit AC1 (1, 44). Here, we hypothesized that a type of functional selectivity (or pathway specificity) could be achieved by inhibiting AC1 to mimic the outcome of G protein activation by MOR. As hypothesized, ST034307 and DAMGO displayed additive effects for inhibition of AC1 when combined at submaximal concentrations. Moreover,  $\beta$ -arrestin recruitment to MOR was similar in the presence or absence of ST034307. These data suggested that ST034307 mimics (at least in part) the effects of  $\text{G}\alpha_{i/o}$  protein activation by MOR.

Activation of G proteins by MOR is also linked to opioid dependence (24, 29, 31). Chronic activation of the MOR leads to a cellular adaptive response termed heterologous sensitization (32). Heterologous sensitization is linked to opioid dependence and is characterized by a marked increase in AC activity (29, 31–33). AC1 knockout mice lack many of the behaviors associated with morphine dependence (7, 9). The fact that ST034307 inhibited both the development and the maintenance of MOR-mediated heterologous sensitization of AC1 suggested that AC1 inhibitors can prevent and suppress this adaptive response to chronic activation of the MOR that has been linked to opioid dependence. This idea is consistent with studies examining the effects of NB001 on naltrexone-mediated heterologous sensitization and hyperalgesia (24).

The promising *in vitro* profile of ST034307 led us to explore the activity of ST034307 in an *in vivo* assay to investigate its potential analgesic properties. Previous studies with NB001 suggested that AC1 inhibitors are efficacious in inflammatory pain models (13). Thus, we used a mouse inflammatory pain model in which intraplantar injection of CFA to the mouse's hindpaw induces an intense inflammatory reaction. Similar to DAMGO, intrathecal injections of ST034307 caused significant relief of CFA-mediated inflammatory pain. The response was dose-dependent and returned the mechanical threshold to baseline levels. We carried out this same experimental paradigm in the presence of the nonselective AC activator forskolin. We hypothesized that the addition of forskolin would activate other AC isoforms that are present with AC1 at the site of action of ST034307 and cause an increase in

cAMP. This increase in cAMP should overwhelm the AC1 inhibition caused by ST034307 and prevent its analgesic activity. As expected, forskolin prevented ST034307-mediated relief of inflammatory pain, suggesting that the analgesia observed was due to inhibition of cAMP accumulation by AC1. These results provide additional support, indicating that inhibitors of AC1 may be useful for treating inflammatory pain and potentially chronic pain, either as independent agents or in combination with opioids. When used in combination with opioids, it may be possible to reduce the amount of opioid required to achieve pain relief and prevent cellular changes associated with opioid dependence and thus extend the usefulness of this class of analgesic agents.

Although previous studies suggest that selective inhibition of AC1 would not cause serious memory impairments (5, 6, 13), additional behavioral assays to examine the effects of small-molecule inhibitors of AC1 on learning and memory should be conducted. The potential of AC1 inhibitors for treating opioid dependence is another interesting avenue that could be explored. Our discovery of a selective AC1 inhibitor (ST034307) should fuel and provide part of the necessary tools for such efforts. The studies conducted herein corroborate the utility of ACs as potential drug targets. We identified a potent small-molecule inhibitor of AC1, and this compound displayed analgesic properties in a model of inflammatory pain.

## MATERIALS AND METHODS

### Compounds and other chemicals used

Forskolin and PMA were purchased from Tocris. Hepes and EDTA were purchased from Fisher Scientific. NKY80 was purchased from EMD Millipore. Isoproterenol, A23187, ATP, EGTA, 3-isobutyl-1-methylxanthine (IBMX), 5'-guanylyl-imidodiphosphate (GppNHp), Tween 20, MgCl<sub>2</sub>, and tris were purchased from Sigma-Aldrich. 2-Bromo-1-(1-phenyl-4,5-dihydro-1H-benzo[d]azepin-3(2H)-yl)ethanone (W400), 6-chloro-2-(trichloromethyl)-4H-chromen-4-one (ST034307), and 4-chloro-1-methyl-3-nitroquinolin-2(1H)-one (ST072383) were purchased from TimTec, and the structures of the compounds were confirmed by nuclear magnetic resonance spectroscopy.

### Cell culture

HEK cells stably expressing AC1, AC8, or AC1 with the MOR were cultured in high-glucose (4500 mg/liter) Dulbecco's modified Eagle's medium containing L-glutamine and sodium pyruvate (Life Technologies) supplemented with 5% bovine calf serum (HyClone), 5% fetal clone I (HyClone), antibiotic-antimycotic (Life Technologies), and G418 (Invivogen) (HEK-AC1) or hygromycin B (Fisher Scientific) (HEK-AC8) or G418 and puromycin (Sigma-Aldrich) (HEK-AC1/MOR). CHO cells expressing the MOR (CHO-MOR) in the PathHunter  $\beta$ -arrestin GPCR assay platform were purchased from DiscoverX. Cells were grown in Ham's F12 medium supplemented with 1 mM L-glutamine (Thermo Scientific), 10% fetal bovine serum (HyClone), penicillin (50 U/ml), streptomycin (50  $\mu$ g/ml) (Life Technologies), G418, and hygromycin B. Cells were grown and frozen as previously described (53).

### Transient transfections

HEK cells were plated in 15-cm dishes at a confluence of  $9.0 \times 10^6$  cells per dish and incubated at 37°C in a humidified incubator overnight. On the following day, a 6-ml solution containing 9  $\mu$ g of AC plasmid or Venus fluorescent protein (Venus) control plasmid and 60  $\mu$ l of Lipofectamine 2000 (Life Technologies) in Opti-MEM

(Life Technologies) was prepared and incubated at room temperature for 45 min. The solution was added dropwise to the cells, and transfection was carried out for 48 hours. Cells were harvested and cryopreserved as described above. For AC7 and AC9, HEK cells were plated in 10-cm dishes (at confluences of  $3.0 \times 10^6$  or  $3.5 \times 10^6$  cells per dish, respectively) and incubated at 37°C in a humidified incubator overnight. On the following day, a 3-ml solution containing AC7 plasmid (10  $\mu$ g), AC9 plasmid (3  $\mu$ g), or Venus plasmid plus G $\alpha_s$  plasmid (0.5  $\mu$ g for AC7 and 0.3  $\mu$ g for AC9) or Venus plasmid and Lipofectamine 2000 (48  $\mu$ l for AC7 and 24  $\mu$ l for AC9) in Opti-MEM was prepared and incubated at room temperature for 45 min. The solution was added dropwise to the cells, transfection was carried out for 48 hours, and cells were harvested and cryopreserved.

### cAMP accumulation in cells

We measured cAMP accumulation as previously described (46). Briefly, cryopreserved cells were thawed, resuspended in Opti-MEM (Life Technologies), and plated in white, flat-bottom, low-volume, tissue culture-treated 384-well plates (PerkinElmer). Plates with cells were incubated in a 37°C humidified incubator for 1 hour. Inhibitors were added, and plates were incubated at room temperature for 30 min followed by the addition of AC stimulants in the presence of 500  $\mu$ M IBMX (phosphodiesterase inhibitor). Cells were incubated at room temperature for 1 hour, and cAMP accumulation was measured using Cisbio's cAMP kit (Cisbio Bioassays) according to the manufacturer's instructions. For the pertussis toxin experiment, HEK-AC1 cells were incubated for 16 hours in the absence or presence of pertussis toxin (25 ng/ml) (Sigma). The cells were then incubated with 30  $\mu$ M ST034307 for 30 min at room temperature, followed by the AC1 stimulation and cAMP quantification. For the CD8- $\beta$ ARK-CT experiment, HEK cells were plated in a six-well plate at a cell density of  $5.5 \times 10^5$  cells per well. After 24 hours of plating, the cells were transiently transfected for 48 hours with AC1 plus Venus (control) or CD8- $\beta$ ARK-CT in a 1:2 (AC1 plasmid/Venus or CD8- $\beta$ ARK-CT plasmid) ratio. The cells were harvested, cryopreserved, and assayed as described above. Additional assays measured cAMP accumulation using the HitHunter cAMP Assay Platform from DiscoverX according to the manufacturer's instructions. Luminescence (HitHunter cAMP assay) and fluorescence (Cisbio's dynamic 2 kit) counts were measured using Synergy 4 (BioTek).

### Compound screening

Cryopreserved HEK-AC1 cells were thawed, washed, resuspended in Opti-MEM, and plated into white, flat-bottom, tissue culture-treated 384-well plates (PerkinElmer) at 15  $\mu$ l per well using a MultiFlo dispenser (BioTek). Cells were incubated in a 37°C humidified incubator for 1 hour. Next, test compounds (3.5 mg/liter final assay concentration) from the NDL-3000 Natural Derivatives Library (TimTec) were added (70 nl per well) using a Multipipette-mounted 384-well pin tool and incubated at room temperature for 30 min. After the incubation with test compounds, 5  $\mu$ l per well of 3  $\mu$ M A23187 in the presence of 30 nM forskolin and 500  $\mu$ M IBMX (final concentrations) was added to the cells using a MultiFlo dispenser. Cells were incubated at room temperature for 1 hour, and cAMP accumulation was measured as described above using a MultiFlo dispenser to sequentially add 10  $\mu$ l per well of cAMP-d2 and anti-cAMP cryptate conjugate working solutions (Cisbio Bioassays) to the cells. Average maximum cAMP values in the presence of the stimulants A23187 and forskolin were  $187 \pm 2.2$  nM, and minimum values (stimulants in the presence of W400) were  $19.4 \pm 0.3$  nM during the screening campaign. Test

compounds were screened in singlet, and a  $Z'$  factor of  $0.55 \pm 0.22$  ( $n = 10$ ) was obtained using  $30 \mu\text{M}$  W400 as a positive control (15, 16).

### Cell viability assays

Cell viability assays were conducted with HEK-AC1 cells following plating and compound incubation protocols identical to the procedures described in “cAMP accumulation in cells.” Cell viability was measured as a percentage of vehicle using 2% Triton X-100 (Sigma-Aldrich) as a control. The CellTiter-Glo Luminescent Cell Viability Assay kit from Promega was used to assess cell viability according to the manufacturer’s instructions. Luminescence counts were measured using Synergy 4.

### cAMP accumulation in cellular membranes from HEK cells

Cellular membranes from HEK-AC1 cells were isolated and frozen as previously described in the presence of 1 mM EGTA (46). On the assay day, membranes were thawed on ice and resuspended in membrane buffer [33 mM Hepes, 0.1% Tween 20, and 1 mM EGTA (pH 7.4)]. Protein concentration was measured using the Pierce BCA Protein Assay kit (Thermo Scientific), and 2.0 to 3.5  $\mu\text{g}$  per well were plated in a white, flat-bottom, tissue culture–treated 384-well plate. Inhibitors (diluted in a 33 mM Hepes and 0.1% Tween 20 solution) were added and incubated for 20 min at room temperature. Next,  $3 \mu\text{M}$  calmodulin or  $30 \mu\text{M}$  forskolin (final concentrations) was added in stimulation buffer (33 mM Hepes, 0.1% Tween 20, 1.5 mM  $\text{MgCl}_2$ , 250  $\mu\text{M}$  ATP, 1  $\mu\text{M}$  GppNHp, 500  $\mu\text{M}$  IBMX, and 500  $\mu\text{M}$   $\text{CaCl}_2/10 \mu\text{M}$  free  $\text{Ca}^{2+}$ ) and incubated at room temperature for 45 min. cAMP accumulation was measured using Cisbio’s dynamic 2 kit according to the manufacturer’s instructions.

### AC assays in cellular membranes from Sf9 cells

Membranes from Sf9 cells expressing AC1, AC2, or AC5 were prepared as previously described (54). All activity assays were performed for 10 min at  $30^\circ\text{C}$  in a final volume of 50  $\mu\text{l}$ . The final concentration of  $\text{MgCl}_2$  and Mg-ATP in the reaction was 10 mM and 200  $\mu\text{M}$ , respectively. AC-containing membranes (10 to 20  $\mu\text{g}$ ) were premixed with  $\text{G}\alpha_s$  (final concentration, 50 nM). Inhibitors were solubilized in dimethyl sulfoxide (DMSO) and incubated with AC-containing membranes for 10 min on ice before the start of the reaction. The final concentration of DMSO in the reaction did not exceed 3% for either vehicle or inhibitors. Reactions were initiated upon addition of a reaction mix containing [ $\alpha$ - $^{32}\text{P}$ ]ATP. The reactions were terminated with stop solution (2.5% SDS, 50 mM ATP, and 1.75 mM cAMP), and the products were separated by sequential chromatography on Dowex-50 and  $\text{Al}_2\text{O}_3$  (54).

### Assays with hippocampal homogenates

C57BL/6 mice (13 weeks old) were decapitated, their brains were quickly removed, and 2-mm slices encompassing the hippocampus were collected on ice. The hippocampal region was dissected and immediately frozen in a  $-80^\circ\text{C}$  freezer, where they were stored until the assay day. Dissected hippocampal tissue was thawed on ice, weighed, and homogenized in membrane buffer (wet weight, 2 ml/mg) with 10 manual strokes using a Wheaton-Teflon glass homogenizer. Homogenates were added to a white, flat-bottom, tissue culture–treated 384-well plate, and inhibitors (diluted in a 33 mM Hepes and 0.1% Tween 20 solution) were added and incubated for 20 min at room temperature. Next,  $3 \mu\text{M}$  calmodulin (final concentration) was added

in stimulation buffer (same as assays in cellular membranes from HEK cells) and incubated at room temperature for 45 min. cAMP accumulation was measured using Cisbio’s dynamic 2 kit according to the manufacturer’s instructions.

### $\beta$ -Arrestin recruitment assay

Recruitment of  $\beta$ -arrestin 2 to the MOR was measured as previously described (46). Briefly, CHO-MOR cells (DiscoverX) were plated in white, flat-bottom, low-volume, tissue culture–treated 384-well plates. Plates with cells were incubated in a  $37^\circ\text{C}$  humidified incubator overnight. After the incubation, AC1 inhibitors or vehicle was added to the cells, which were incubated at room temperature for 30 min. Next, DAMGO or vehicle was added to the cells, which were then incubated in a  $37^\circ\text{C}$  humidified incubator for 1.5 hours.  $\beta$ -Arrestin 2 recruitment to the MOR was assessed using the PathHunter assay (DiscoverX) according to the manufacturer’s instructions. Luminescence counts were measured using Synergy 4.

### Heterologous sensitization assays

Heterologous sensitization assays were conducted as previously described (55). Briefly, HEK-AC1/MOR cells were thawed and plated in white, flat-bottom, tissue culture–treated 384-well plates. Plates with cells were incubated in a  $37^\circ\text{C}$  humidified incubator for 1 hour. For inhibition of the development of sensitization, inhibitors were added, and plates were incubated at room temperature for 30 min, followed by addition of DAMGO and incubation at  $37^\circ\text{C}$  for 2 hours (to achieve sensitization). For the assays to measure inhibition of the maintenance of sensitization, the order of DAMGO and ST034307 additions was reversed (DAMGO sensitization before AC1 inhibition). Next, cells were treated with  $3 \mu\text{M}$  A23187 in the presence of 500  $\mu\text{M}$  IBMX and 1  $\mu\text{M}$  naloxone (final concentrations) and incubated at room temperature for 1 hour. cAMP accumulation was measured using Cisbio’s dynamic 2 kit according to the manufacturer’s instructions.

### Animals and housing

Wild-type C57BL/6 mice were obtained from Taconic. Male mice aged 5 weeks (18 to 23 g) were grouped and housed in single-grommet ventilated Plexiglas cages at ambient temperature ( $21^\circ\text{C}$ ) in a room maintained on a reversed 12-hour light/12-hour dark cycle (lights off at 1000, lights on at 2200) in our animal facility approved by the Association for Assessment and Accreditation of Laboratory Animal Care. Food and water were provided ad libitum. The mice were given  $\sim 7$  days to acclimatize to the housing conditions and reverse light cycle before the start of the experiments. Mice were then habituated to the containment boxes for the von Frey assay. All animal procedures were preapproved by our Institutional Animal Care and Use Committee and were in accordance with the National Institutes of Health’s *Guide for the Care and Use of Laboratory Animals*. Mice were not deprived of food or water at any time.

### Inflammatory pain behavioral assays

C57BL/6 mice were placed in suspended rectangular plastic chambers on a wire mesh grid to habituate for 1 hour. Next, a baseline measurement of mechanical sensitivity to von Frey filaments was performed as previously described (24, 34). Immediately after baseline measurements, the mice were injected with CFA (10  $\mu\text{l}$ , nondiluted) into the intraplantar surface of the left hindpaw to induce inflammation (24). On the following day, inflammatory hypersensitivity was measured using von Frey filaments. Next, drugs were injected intrathecaally as previously



described (34). Drug-induced analgesia was measured 10 min after intrathecal injections using von Frey filaments. Data are represented as a percentage of the average baseline response.

### Data and statistical analyses

All data and statistical analyses were carried out using GraphPad Prism 6 (GraphPad Software). Statistical analyses (one-sample *t* test, one-way ANOVA, or two-way ANOVA) are described in text or figure legends where appropriate.

### SUPPLEMENTARY MATERIALS

[www.sciencesignaling.org/cgi/content/full/10/467/eaah5381/DC1](http://www.sciencesignaling.org/cgi/content/full/10/467/eaah5381/DC1)

Fig. S1. Inhibitory activity of ST034307 and NB001 against AC1.

Fig. S2. Inhibitory activity of ST034307 after pertussis toxin treatment or sequestration of G $\beta$ y.

Fig. S3. A23187- and forskolin-stimulated cAMP accumulation in HEK-AC1 cells.

Table S1. Inhibition of A23187-stimulated AC1 activity using two different methods of measuring cAMP accumulation.

Data S1. ND1-3000 screen results.

### REFERENCES AND NOTES

- D. M. F. Cooper, A. J. Crossthwaite, Higher-order organization and regulation of adenylyl cyclases. *Trends Pharmacol. Sci.* **27**, 426–431 (2006).
- R. K. Sunahara, R. Taussig, Isoforms of mammalian adenylyl cyclase: Multiplicities of signaling. *Mol. Interv.* **2**, 168–184 (2002).
- R. Sadana, C. W. Dessauer, Physiological roles for G protein-regulated adenylyl cyclase isoforms: Insights from knockout and overexpression studies. *Neurosignals* **17**, 5–22 (2009).
- G. D. Ferguson, D. R. Storm, Why calcium-stimulated adenylyl cyclases? *Physiology* **19**, 271–276 (2004).
- S. T. Wong, J. Athos, X. A. Figueroa, V. V. Pineda, M. L. Schaefer, C. C. Chavkin, L. J. Muglia, D. R. Storm, Calcium-stimulated adenylyl cyclase activity is critical for hippocampus-dependent long-term memory and late phase LTP. *Neuron* **23**, 787–798 (1999).
- Q. Shan, G. C.-K. Chan, D. R. Storm, Type 1 adenylyl cyclase is essential for maintenance of remote contextual fear memory. *J. Neurosci.* **28**, 12864–12867 (2008).
- S. Li, M. L. Lee, M. R. Bruchas, G. C. Chan, D. R. Storm, C. Chavkin, Calmodulin-stimulated adenylyl cyclase gene deletion affects morphine responses. *Mol. Pharmacol.* **70**, 1742–1749 (2006).
- K. I. Vadakkan, H. Wang, S. W. Ko, E. Zastepa, M. J. Petrovic, K. A. Sluka, M. Zhuo, Genetic reduction of chronic muscle pain in mice lacking calcium/calmodulin-stimulated adenylyl cyclases. *Mol. Pain* **2**, 7 (2006).
- V. Zachariou, R. Liu, Q. LaPlant, G. Xiao, W. Renthal, G. C. Chan, D. R. Storm, G. Aghajanian, E. J. Nestler, Distinct roles of adenylyl cyclases 1 and 8 in opiate dependence: Behavioral, electrophysiological, and molecular studies. *Biol. Psychiatry* **63**, 1013–1021 (2008).
- M. Zhuo, Targeting neuronal adenylyl cyclase for the treatment of chronic pain. *Drug Discov. Today* **17**, 573–582 (2012).
- F. Wei, K. I. Vadakkan, H. Toyoda, L.-J. Wu, M.-G. Zhao, H. Xu, F. W. F. Shum, Y. H. Jia, M. Zhuo, Calcium calmodulin-stimulated adenylyl cyclases contribute to activation of extracellular signal-regulated kinase in spinal dorsal horn neurons in adult rats and mice. *J. Neurosci.* **26**, 851–861 (2006).
- H. Xu, L.-J. Wu, H. Wang, X. Zhang, K. I. Vadakkan, S. S. Kim, H. W. Steenland, M. Zhuo, Presynaptic and postsynaptic amplifications of neuropathic pain in the anterior cingulate cortex. *J. Neurosci.* **28**, 7445–7453 (2008).
- H. Wang, H. Xu, L.-J. Wu, S. S. Kim, T. Chen, K. Koga, G. Descalzi, B. Gong, K. I. Vadakkan, X. Zhang, B.-K. Kaang, M. Zhuo, Identification of an adenylyl cyclase inhibitor for treating neuropathic and inflammatory pain. *Sci. Transl. Med.* **3**, 65ra63 (2011).
- C. S. Brand, H. J. Hocker, A. A. Gorfe, C. N. Cavasotto, C. W. Dessauer, Isoform selectivity of adenylyl cyclase inhibitors: Characterization of known and novel compounds. *J. Pharmacol. Exp. Ther.* **347**, 265–275 (2013).
- J. M. Conley, C. S. Brand, A. S. Bogard, E. P. S. Pratt, R. Xu, G. H. Hockerman, R. S. Ostrom, C. W. Dessauer, V. J. Watts, Development of a high-throughput screening paradigm for the discovery of small-molecule modulators of adenylyl cyclase: Identification of an adenylyl cyclase 2 inhibitor. *J. Pharmacol. Exp. Ther.* **347**, 276–287 (2013).
- J.-H. Zhang, T. D. Chung, K. R. Oldenburg, A simple statistical parameter for use in evaluation and validation of high throughput screening assays. *J. Biomol. Screen.* **4**, 67–73 (1999).
- P. W. Iversen, B. Beck, Y. F. Chen, W. Dere, V. Devanarayan, B. J. Eastwood, M. W. Farnen, S. J. Iturria, C. Montrose, R. A. Moore, J. R. Weidner, G. S. Sittampalam, in *Assay Guidance Manual*, G. S. Sittampalam, N. P. Coussens, H. Nelson, M. Arkin, D. Auld, C. Austin, B. Bejcek, M. Glucksman, J. Inglese, P. W. Iversen, Z. Li, J. McGee, O. McManus, L. Minor, A. Napper, J. M. Peltier, T. Riss, O. J. Trask Jr., J. Weidner, Eds. (Eli Lilly & Company and the National Center for Advancing Translational Sciences, 2004).
- K. B. Seamon, J. W. Daly, Forskolin: A unique diterpene activator of cyclic AMP-generating systems. *J. Cyclic Nucleotide Res.* **7**, 201–224 (1981).
- M. G. Cumbay, V. J. Watts, Heterologous sensitization of recombinant adenylyl cyclases by activation of D<sub>2</sub> dopamine receptors. *J. Pharmacol. Exp. Ther.* **297**, 1201–1209 (2001).
- M.-G. Ludwig, K. Seuwen, Characterization of the human adenylyl cyclase gene family: cDNA, gene structure, and tissue distribution of the nine isoforms. *J. Recept. Signal Transduct. Res.* **22**, 79–110 (2002).
- A. V. Smrcka, D. M. Lehmann, A. L. Dessal, G protein  $\beta$  subunits as targets for small molecule therapeutic development. *Comb. Chem. High Throughput Screen.* **11**, 382–395 (2008).
- C. W. Dessauer, J. J. G. Tesmer, S. R. Sprang, A. G. Gilman, The interactions of adenylyl cyclases with P-site inhibitors. *Trends Pharmacol. Sci.* **20**, 205–210 (1999).
- R. Seifert, G. H. Lushington, T.-C. Mou, A. Gille, S. R. Sprang, Inhibitors of membranous adenylyl cyclases. *Trends Pharmacol. Sci.* **33**, 64–78 (2012).
- G. Corder, S. Doolen, R. R. Donahue, M. K. Winter, B. L. Jutras, Y. He, X. Hu, J. S. Wieskopf, J. S. Mogil, D. R. Storm, Z. J. Wang, K. E. McCarson, B. K. Taylor, Constitutive  $\mu$ -opioid receptor activity leads to long-term endogenous analgesia and dependence. *Science* **341**, 1394–1399 (2013).
- A. K. P. Jones, L. Y. Qi, T. Fujirawa, S. K. Luthra, J. Ashburner, P. Bloomfield, V. J. Cunningham, M. Itoh, H. Fukuda, T. Jones, In vivo distribution of opioid receptors in man in relation to the cortical projections of the medial and lateral pain systems measured with positron emission tomography. *Neurosci. Lett.* **126**, 25–28 (1991).
- A. Mansour, C. A. Fox, H. Akil, S. J. Watson, Opioid-receptor mRNA expression in the rat CNS: Anatomical and functional implications. *Trends Neurosci.* **18**, 22–29 (1995).
- A. Mansour, H. Khachaturian, M. E. Lewis, H. Akil, S. J. Watson, Anatomy of CNS opioid receptors. *Trends Neurosci.* **11**, 308–314 (1988).
- K. M. Raehal, L. M. Bohn,  $\beta$ -Arrestins: Regulatory role and therapeutic potential in opioid and cannabinoid receptor-mediated analgesia. *Handb. Exp. Pharmacol.* **219**, 427–443 (2014).
- L. M. Bohn, R. R. Gainetdinov, F.-T. Lin, R. J. Lefkowitz, M. G. Caron,  $\mu$ -Opioid receptor desensitization by  $\beta$ -arrestin-2 determines morphine tolerance but not dependence. *Nature* **408**, 720–723 (2000).
- M. J. Clark, R. R. Neubig, J. R. Traynor, Endogenous regulator of G protein signaling proteins suppress G $\alpha$ o-dependent,  $\mu$ -opioid agonist-mediated adenylyl cyclase supersensitization. *J. Pharmacol. Exp. Ther.* **310**, 215–222 (2004).
- V. J. Watts, K. A. Neve, Sensitization of adenylyl cyclase by G $\alpha_{i/o}$ -coupled receptors. *Pharmacol. Ther.* **106**, 405–421 (2005).
- T. F. Brust, J. M. Conley, V. J. Watts, G $\alpha_{i/o}$ -coupled receptor-mediated sensitization of adenylyl cyclase: 40 years later. *Eur. J. Pharmacol.* **763**, 223–232 (2015).
- S. K. Sharma, W. A. Klee, M. Nirenberg, Dual regulation of adenylyl cyclase accounts for narcotic dependence and tolerance. *Proc. Natl. Acad. Sci. U.S.A.* **72**, 3092–3096 (1975).
- R. M. van Rijn, D. I. Brissett, J. L. Whistler, Emergence of functional spinal delta opioid receptors after chronic ethanol exposure. *Biol. Psychiatry* **71**, 232–238 (2012).
- H. Wang, B. Gong, K. I. Vadakkan, H. Toyoda, B.-K. Kaang, M. Zhuo, Genetic evidence for adenylyl cyclase 1 as a target for preventing neuronal excitotoxicity mediated by N-methyl-D-aspartate receptors. *J. Biol. Chem.* **282**, 1507–1517 (2007).
- F. Wei, C.-S. Qiu, S. J. Kim, L. Muglia, J. W. Maas Jr., V. V. Pineda, H.-M. Xu, Z.-F. Chen, D. R. Storm, L. J. Muglia, M. Zhuo, Genetic elimination of behavioral sensitization in mice lacking calmodulin-stimulated adenylyl cyclases. *Neuron* **36**, 713–726 (2002).
- T. T. Wager, X. Hou, P. R. Verhoest, A. Villalobos, Moving beyond rules: The development of a central nervous system multiparameter optimization (CNS MPO) approach to enable alignment of druglike properties. *ACS Chem. Neurosci.* **1**, 435–449 (2010).
- C. Pinto, D. Papa, M. Hübner, T.-C. Mou, G. H. Lushington, R. Seifert, Activation and inhibition of adenylyl cyclase isoforms by forskolin analogs. *J. Pharmacol. Exp. Ther.* **325**, 27–36 (2008).
- S. Pierre, T. Eschenhagen, G. Geisslinger, K. Scholich, Capturing adenylyl cyclases as potential drug targets. *Nat. Rev. Drug Discov.* **8**, 321–335 (2009).
- R. Berdeau, R. Stewart, cAMP signaling in skeletal muscle adaptation: Hypertrophy, metabolism, and regeneration. *Am. J. Physiol. Endocrinol. Metab.* **303**, E1–E17 (2012).
- C. E. Torgan, W. E. Kraus, Regulation of type II adenylyl cyclase mRNA in rabbit skeletal muscle by chronic motor nerve pacing. *Am. J. Physiol.* **271**, E253–E260 (1996).

42. K. M. Raehal, C. L. Schmid, C. E. Groer, L. M. Bohn, Functional selectivity at the  $\mu$ -opioid receptor: Implications for understanding opioid analgesia and tolerance. *Pharmacol. Rev.* **63**, 1001–1019 (2011).
43. J. D. Violin, A. L. Crombie, D. G. Soergel, M. W. Lark, Biased ligands at G-protein-coupled receptors: Promise and progress. *Trends Pharmacol. Sci.* **35**, 308–316 (2014).
44. C. Lüscher, P. A. Slesinger, Emerging roles for G protein-gated inwardly rectifying potassium (GIRK) channels in health and disease. *Nat. Rev. Neurosci.* **11**, 301–315 (2010).
45. J. T. Williams, S. L. Ingram, G. Henderson, C. Chavkin, M. von Zastrow, S. Schulz, T. Koch, C. J. Evans, M. J. Christie, Regulation of  $\mu$ -opioid receptors: Desensitization, phosphorylation, internalization, and tolerance. *Pharmacol. Rev.* **65**, 223–254 (2013).
46. T. F. Brust, M. P. Hayes, D. L. Roman, K. D. Burris, V. J. Watts, Bias analyses of preclinical and clinical D<sub>2</sub> dopamine ligands: Studies with immediate and complex signaling pathways. *J. Pharmacol. Exp. Ther.* **352**, 480–493 (2015).
47. J. D. Urban, W. P. Clarke, M. von Zastrow, D. E. Nichols, B. Kobilka, H. Weinstein, J. A. Javitch, B. L. Roth, A. Christopoulos, P. M. Sexton, K. J. Miller, M. Spedding, R. B. Mailman, Functional selectivity and classical concepts of quantitative pharmacology. *J. Pharmacol. Exp. Ther.* **320**, 1–13 (2007).
48. E. J. Whalen, S. Rajagopal, R. J. Lefkowitz, Therapeutic potential of  $\beta$ -arrestin- and G protein-biased agonists. *Trends Mol. Med.* **17**, 126–139 (2011).
49. Z. Rankovic, T. F. Brust, L. M. Bohn, Biased agonism: An emerging paradigm in GPCR drug discovery. *Bioorg. Med. Chem. Lett.* **26**, 241–250 (2016).
50. L. M. Bohn, L. A. Dykstra, R. J. Lefkowitz, M. G. Caron, L. S. Barak, Relative opioid efficacy is determined by the complements of the G protein-coupled receptor desensitization machinery. *Mol. Pharmacol.* **66**, 106–112 (2004).
51. L. M. Bohn, R. J. Lefkowitz, R. R. Gainetdinov, K. Peppel, M. G. Caron, F. T. Lin, Enhanced morphine analgesia in mice lacking  $\beta$ -arrestin 2. *Science* **286**, 2495–2498 (1999).
52. K. M. Raehal, J. K. L. Walker, L. M. Bohn, Morphine side effects in  $\beta$ -arrestin 2 knockout mice. *J. Pharmacol. Exp. Ther.* **314**, 1195–1201 (2005).
53. J. M. Conley, T. F. Brust, R. Xu, K. D. Burris, V. J. Watts, Drug-induced sensitization of adenylyl cyclase: Assay streamlining and miniaturization for small molecule and siRNA screening applications. *J. Vis. Exp.* **2014**, e51218 (2014).
54. C. W. Dessauer, Kinetic analysis of the action of P-site analogs. *Methods Enzymol.* **345**, 112–126 (2002).
55. T. F. Brust, M. P. Hayes, D. L. Roman, V. J. Watts, New functional activity of aripiprazole revealed: Robust antagonism of D2 dopamine receptor-stimulated G $\beta\gamma$  signaling. *Biochem. Pharmacol.* **93**, 85–91 (2015).

**Acknowledgments:** We thank J. M. Conley for assistance with the development of the screening platform, T. Kinzer-Ursen for providing purified calmodulin, and T. Chiang for assistance with tissue collection and dissections. We also acknowledge B. Craig, M. Liu, and the Purdue Statistical Consulting Services for statistical advice. **Funding:** This research was supported by grants R01 MH060397 and R21 MH101673 from the National Institute of Mental Health, a Purdue Showalter Trust Award, and the Purdue Research Foundation. **Author contributions:** T.F.B., D.A., M.S.-V., T.A.B., and Z.Y. conducted experiments; T.F.B., M.S.-V., R.M.v.R., C.W.D., M.D., and V.J.W. developed the experimental design; T.F.B., M.D., R.M.v.R., and V.J.W. performed data analyses; and T.F.B., M.D., C.W.D., R.M.v.R., and V.J.W. contributed to writing of the manuscript. **Competing interests:** The authors declare that they have no competing interests.

Submitted 12 July 2016

Accepted 30 January 2017

Published 21 February 2017

10.1126/scisignal.aah5381

**Citation:** T. F. Brust, D. Alongkronrasmee, M. Soto-Velasquez, T. A. Baldwin, Z. Ye, M. Dai, C. W. Dessauer, R. M. van Rijn, V. J. Watts, Identification of a selective small-molecule inhibitor of type 1 adenylyl cyclase activity with analgesic properties. *Sci. Signal.* **10**, eaah5381 (2017).

## Identification of a selective small-molecule inhibitor of type 1 adenylyl cyclase activity with analgesic properties

Tarsis F. Brust, Dounkamol Alongkronrusmee, Monica Soto-Velasquez, Tanya A. Baldwin, Zhishi Ye, Mingji Dai, Carmen W. Dessauer, Richard M. van Rijn and Val J. Watts

*Sci. Signal.* **10** (467), eaah5381.  
DOI: 10.1126/scisignal.aah5381

### Pain relief through AC1 inhibition

Brust *et al.* identified a small-molecule inhibitor of adenylyl cyclase 1 (AC1), which is a potential target for treating pain and reducing the dependency on opioids for pain management. The challenge has been that there are many AC isoforms and their function is crucial to most physiological processes, so isoform specificity is key to any chance of therapeutic efficacy. The authors identified two compounds that inhibited AC1 in a screen of a chemical library of natural compounds that reduced the production of adenosine 3',5'-monophosphate (cAMP), the product of AC activity. One of the compounds, ST034307, showed selective inhibition of AC1 over all eight other AC isoforms. This compound produced analgesia in a mouse model of inflammatory pain, blocked cellular changes associated with opioid dependency in transfected cells, and inhibited cAMP accumulation in both transfected cells and hippocampal tissue samples. This compound should not only be a useful tool for investigating AC1-specific physiology but also provide support for the development of AC1-selective pain relievers.

ARTICLE TOOLS	<a href="http://stke.sciencemag.org/content/10/467/eaah5381">http://stke.sciencemag.org/content/10/467/eaah5381</a>
SUPPLEMENTARY MATERIALS	<a href="http://stke.sciencemag.org/content/suppl/2017/02/16/10.467.eaah5381.DC1">http://stke.sciencemag.org/content/suppl/2017/02/16/10.467.eaah5381.DC1</a>
RELATED CONTENT	<a href="http://stke.sciencemag.org/content/sigtrans/10/461/eaah4874.full">http://stke.sciencemag.org/content/sigtrans/10/461/eaah4874.full</a> <a href="http://stm.sciencemag.org/content/scitransmed/3/65/65ra3.full">http://stm.sciencemag.org/content/scitransmed/3/65/65ra3.full</a> <a href="http://stke.sciencemag.org/content/sigtrans/10/485/eaao1782.full">http://stke.sciencemag.org/content/sigtrans/10/485/eaao1782.full</a> <a href="http://stke.sciencemag.org/content/sigtrans/10/488/eaao3722.full">http://stke.sciencemag.org/content/sigtrans/10/488/eaao3722.full</a> <a href="http://stke.sciencemag.org/content/sigtrans/11/520/eaah3738.full">http://stke.sciencemag.org/content/sigtrans/11/520/eaah3738.full</a> <a href="http://stke.sciencemag.org/content/sigtrans/11/523/eaar4394.full">http://stke.sciencemag.org/content/sigtrans/11/523/eaar4394.full</a> <a href="http://stke.sciencemag.org/content/sigtrans/11/535/eaao3134.full">http://stke.sciencemag.org/content/sigtrans/11/535/eaao3134.full</a> <a href="http://stke.sciencemag.org/content/sigtrans/11/552/eaao5150.full">http://stke.sciencemag.org/content/sigtrans/11/552/eaao5150.full</a>
REFERENCES	This article cites 54 articles, 19 of which you can access for free <a href="http://stke.sciencemag.org/content/10/467/eaah5381#BIBL">http://stke.sciencemag.org/content/10/467/eaah5381#BIBL</a>
PERMISSIONS	<a href="http://www.sciencemag.org/help/reprints-and-permissions">http://www.sciencemag.org/help/reprints-and-permissions</a>

Use of this article is subject to the [Terms of Service](#)

*Science Signaling* (ISSN 1937-9145) is published by the American Association for the Advancement of Science, 1200 New York Avenue NW, Washington, DC 20005. The title *Science Signaling* is a registered trademark of AAAS.

Copyright © 2017, American Association for the Advancement of Science